Extreme Mechanics Letters 18 (2018) 1–8

Contents lists available at ScienceDirect

Extreme Mechanics Letters

journal homepage: www.elsevier.com/locate/eml

Compressible hexagonal-structured triboelectric nanogenerators for harvesting tire rotation energy

Tong Guo [a,b,c,d,1], Guoxu Liu [a,c,d,1], Yaokun Pang [a,c,d], Bo Wu [a,c,d], Fengben Xi [a,c,d], Junqing Zhao [a,c,d], Tianzhao Bu [a,c,d], Xianpeng Fu [a,c,d], Xinjian Li [b,*], Chi Zhang [a,c,d,**], Zhong Lin Wang [a,c,d,e,*]

[a] Beijing Institute of Nanoenergy and Nanosystems, Chinese Academy of Sciences, Beijing 100083, China
[b] Department of Physics and Laboratory of Material Physics, Zhengzhou University, Zhengzhou 450052, China
[c] National Center for Nanoscience and Technology (NCNST), Beijing 100190, China
[d] University of Chinese Academy of Sciences, Beijing 100049, China
[e] School of Materials Science and Engineering, Georgia Institute of Technology, Atlanta, GA 30332-0245, USA

GRAPHICAL ABSTRACT

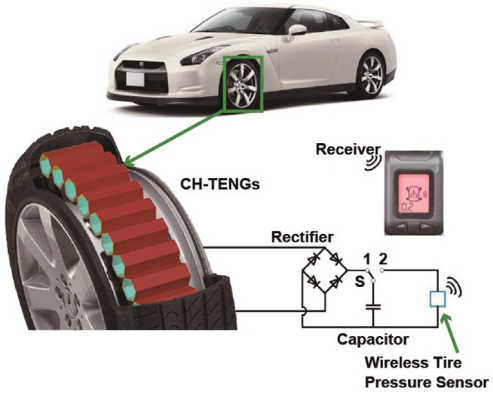

ARTICLE INFO

Article history:
Received 30 August 2017
Received in revised form 24 October 2017
Accepted 27 October 2017
Available online 7 November 2017

Keywords:
Triboelectric nanogenerator
Compressible hexagonal-structure
Energy harvesting
Tire pressure sensor
Automotive electronics

ABSTRACT

Mechanical energy in a rolling tire is strong and stable, but it is always wasted and there is no effective means for harvesting. Herein, we demonstrate an array of compressible hexagonal-structured triboelectric nanogenerators (CH-TENGs) for harvesting the mechanical energy from a rolling tire. The CH-TENG units can be stacked in parallel connections and fixed in a rubber tire. The energy harvesting performances are systematically investigated and the maximum instantaneous power is 1.9 mW with the CH-TENG in 8 units, a weight load of 10 N and a speed of 2.51 m/s. The CH-TENGs have stable and durable characteristics for a 30-day continuous work and can drive a wireless tire pressure sensor once every 14 min when the moving speed is 2.51 m/s and weight load is 10 N. On the basis of the measured output power of the CH-TENG, it is expected to produce at least 1.2 W for a standard tire with the CH-TENG in 500 units and the running speed of 100 km/h. This work not only provides a promising solution to harvest the wasted

* Corresponding authors.
** Corresponding author at: Beijing Institute of Nanoenergy and Nanosystems, Chinese Academy of Sciences, Beijing 100083, China.
E-mail addresses: lixj@zzu.edu.cn (X. Li), czhang@binn.cas.cn (C. Zhang), zlwang@gatech.edu (Z.L. Wang).
[1] T. G. and G. X. L. contributed equally to this work.

https://doi.org/10.1016/j.eml.2017.10.002

mechanical energy from rolling tires, but also demonstrates the potential applications of the CH-TENG in sustainable automotive electronics.

1. Introduction

Tire pressure test system is very important to vehicles' safety, but it needs to be powered by battery [1], which has the limited lifetime and is not environmentally friendly. Mechanical energy widely exists in our living environment and industrial production process, especially in vehicles. Many studies forecast that the Chinese vehicle population will continue to increase to 360–540 million by 2030 [2–4]. Automobile movement, as the wasted mechanical energy, could be probably collected for powering tire pressure test system. It is promising to be an important energy recovery solution for automotive electronics.

Since 2012, the triboelectric nanogenerator (TENG) [5–7] based on the Maxwell's displacement current has been invented to convert ambient mechanical energy into electricity [8]. Owing to the advantages of high output performance [9,10], light-weight [11], low-cost [12], low frequency [13] and easy to fabricate [14], the TENG has greatly impacted the field of energy harvesting [15,16] and information sensing [17–22]. The triboelectric energy harvesting transducers will be a $400 million market in 2027 by the prediction of IDTechEx [23]. So far, the TENG has been widely used in harvesting human kinetic [24–26] and environmental mechanical energy [27], which can also be used to harvest the rotating mechanical energy [28–31] of tires motion [32] as a mainly energy-loss way in vehicles. However, the traditional contacting-separation TENG [33] consists of a pair of thin film materials with metal electrodes and two substrates as supporting materials, which is difficult to match the structure of tires in vehicles. So, it is a challenge that how to design the structure of TENG to match the tires and harvest maximum friction energy of rotating tires for powering automotive electronics.

Here, we demonstrate compressible hexagonal-structured triboelectric nanogenerators (CH-TENGs) for harvesting the mechanical energy from rolling tires, which consist of a FEP (Fluorinated ethylene propylene) film and copper electrodes. When integrated into the structure of tires in vehicles, the CH-TENG has good structural stability and high space utilization, and the CH-TENG units can be stacked in parallel connections like a honeycomb. The energy harvesting performances of CH-TENGs fixed in a rolling tire are systematically investigated. The output performances of CH-TENGs are related to different units, the speed and the weight loads of tires, and the maximum instantaneous power is 1.9 mW with the CH-TENG in 8 units, a weight load of 10 N and a speed of 2.51 m/s. Moreover, the CH-TENGs have stable and durable characteristics for a 30-day continuous work and can drive the wireless tire pressure sensor every 14 min when the moving speed is 2.51 m/s and weight load is 10 N. On the basis of the measured output power of the CH-TENG, it is expected to produce at least 1.2 W for a standard tire with the CH-TENG in 500 units and the running speed of 100 km/h. This work not only provides a promising solution to harvest the wasted mechanical energy from rolling tires, but also demonstrates the potential applications of the CH-TENG in sustainable automotive electronics.

2. Methods

2.1. Fabrication of the CH-TENG

PI (Polyimide) is used to fabricate CH-TENG. First, a straight line that is perpendicular to long side is drawn on a piece of PI (125 μm thick, 70 mm×50 mm) every 10 mm. Second, Two separate copper foils (50 μm thick, 30 mm×50 mm) are closely stuck on the PI. Third, a piece of FEP film (50 μm thick, 30 mm×50 mm) is closely stuck on the either of copper foils. Finally, the CH-TENG is accomplished after sticking.

2.2. Surface modification of the FEP film

First, a piece of FEP film (50 μm thick, 30 mm × 50 mm in area) is cleaned in an ultrasonic cleaner with ethanol and deionized water and is then blow-dried in a drying oven. Before being etched, a layer of Cu is sputtered onto the surface of the FEP, and then O_2, Ar, and CF_4 gases are fed into the ICP (inductive coupling plasma) chamber to etch the surface with flow rates of 10.0, 15.0, and 30.0 sccm, respectively. To generate the plasma, a power source of 400 W is chosen, while another power source (100 W) is used to accelerate plasma ions moving to the FEP surface. With an etching time of 6 min, desired nanostructures are obtained on the Cu-coated FEP surface.

2.3. Characterization of the CH-TENG

The output voltage, current and charge of the CH-TENG are quantitatively measured by a system electrometer (Keithley 6514) at room temperature.

2.4. Demonstration scenario of the CH-TENG

Eight CH-TENGs can be fixed in a rubber tire (70 mm in diameter, 62 mm in width and a load of 6 N). An iron axis locates in the middle of the rubber tire, which rotates with rubber tire rotation. Each CH-TENG is stuck and tangent to the rubber tire. The rubber tire is fixed on the conveyor belt that is driven by an accurate motor. The speed range of the motor is 100∼600 rad/min. To completely contact between the CH-TENGs and the conveyor belt, the sponge with a thickness of 5 mm is covered outside the CH-TENGs. Then, a pair of conductive brushes is fabricated by carbon fibers to connect with the CH-TENGs. There is a pair of acrylic sheets that is covered by copper foils contacting with conductive brushes for transmitting charges of the rolling tire. The rubber tire and acrylic sheets are fixed on the lifting platform which can change the weight load between the tire and the conveyor belt by adjusting the height. In the application scenario, the CH-TENG in 8 units is fixed in the rubber tire and connected with a wireless tire pressure sensor.

3. Results and discussion

3.1. Structure of the CH-TENG

Hexagonal structure is the best topological structure for covering two-dimensional plane, which has the advantages of the highest-degree adaptability, the simplest material consumption and the largest space utilization. Based on the hexagonal structure, we design the CH-TENG for harvesting energy from rolling tires. Fig. 1 shows basic structure of the CH-TENG. The CH-TENG is mainly composed of two copper electrodes, a piece of flexible PI and FEP film, as schemed in Fig. 1a. PI is selected as the material for substrates and is folded into hexagon due to its high strength, light weight, easy processing, and low cost. On the lower side, a layer of

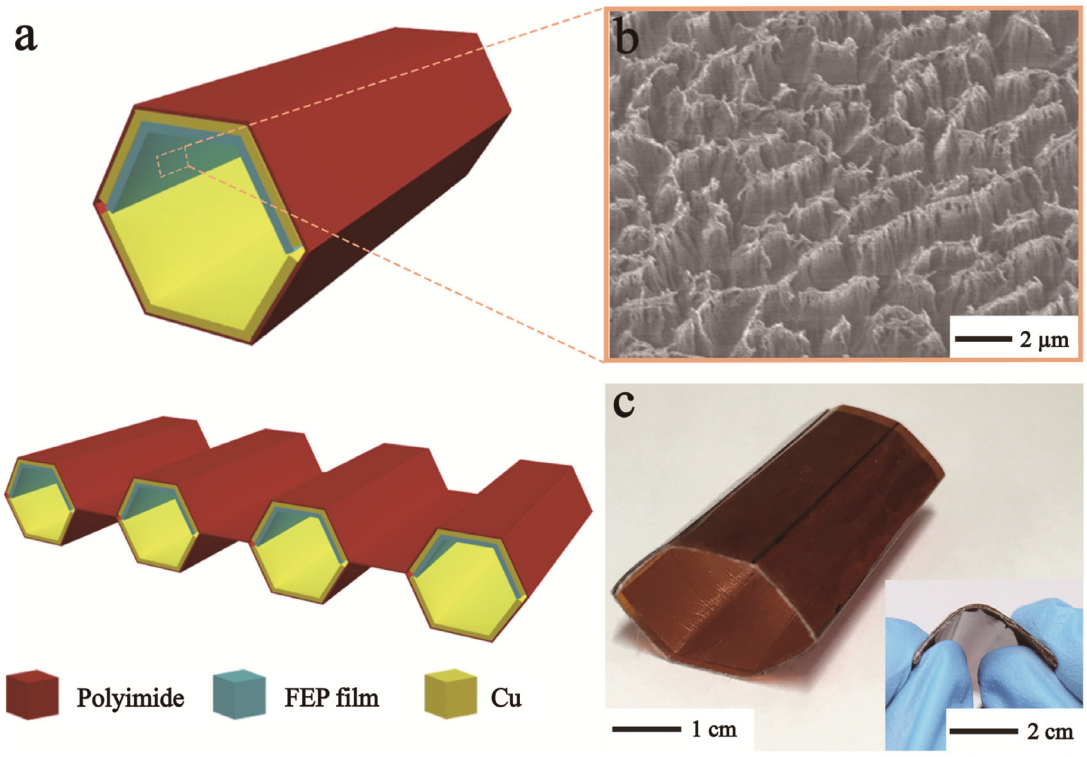

Fig. 1. Basic structure of the CH-TENG. (a) Schematic illustrations of the CH-TENG in single and stack. (b) Scanning electron microscopy image of nanostructures on the surface of the FEP film. (c) Photograph of the CH-TENG. The inset is the CH-TENG bent by hand.

contact electrode is prepared, which plays dual roles of electrode and contact surface. On the other side, a copper electrode is laminated between the substrate and a layer of FEP film. This electrode is called back electrode for later reference. There is a narrow spacing between the contact electrode and the FEP film. As shown in Fig. 1a, the CH-TENG units can be stacked in parallel connections and the structure of different combinations can match different kinds of experimental scenes. In order to optimize the triboelectrification between the two materials, the surface of the FEP film is modified via ICP to create nanostructures, which can enhance the surface triboelectric charge density of the FEP film [19], as shown in Fig. 1b. A well-designed CH-TENG is presented in Fig. 1c and the inset is the photograph of the CH-TENG bend by hand, which shows the great suppleness of the CH-TENG. Hexagonal structure of the CH-TENGs can be stacked into different combinations for different structure of the tires, as shown in **Fig. S1**. The CH-TENG can be fixed in the inner side of the outer tires for power generation by tiny deformation. Compared with previous TENGs in rotational or sliding modes, it is much lighter and easier for integration without any influences on current tire structures and the friction between the tire and road.

3.2. Working principle of the CH-TENG

The working mechanism of the CH-TENG is elaborated in Fig. 2. As is shown in Fig. 2a, there are many CH-TENGs fixed in a tire, which is rotating in counterclockwise direction. The inset is magnified schematic illustration of a CH-TENG. A detailed cycle with six stages for the working process of a CH-TENG is shown in Fig. 2b. The fundamental working principle of a CH-TENG is based on the conjunction of contact electrification and electrostatic induction. It is supposed to be an original stage when the FEP film contacts completely with the contact electrode. According to the triboelectric series [34], in which materials are listed in order of the polarity of charge separation when they are touched with another object, electrons are transferred from the contact electrode to the FEP film, resulting in positive and negative triboelectric charges on the contact electrode and FEP surface, respectively (stage I). When the tire continues rotating, the right part of the CH-TENG starts separating. Because the contact electrode has a higher potential than the back electrode, electrons flow from the back electrode to the contact electrode through the external circuit to neutralize the positive triboelectric charges in the contact electrode (stage II and III). The flow of electrons lasts until the separation is maximized, and an electrostatic equilibrium is reached (stage IV). When the tire rotates after a period, the right part of the CH-TENG will be impacted. Thus, the former electrostatic equilibrium is broken. Electrons flow back from the contact electrode to the back electrode through the external circuit (stage V and VI). Finally, when the contact electrode and FEP film contact with each other again, there is no current flowing in the external circuit (stage I). This is a full cycle of the electricity generation process. As the tire rotating in the environment, electricity is generated. To theoretically predict the distribution of the electrical potential between the two electrodes, COMSOL software that employs the finite element method (FEM) is implemented to model the CH-TENG, as is shown in Fig. 2c. The strain of the CH-TENG in the vertical direction is systematically simulated, as shown in Fig. S2. In a cycle, the initial CH-TENG (stage IV) is fully compressed (stage I) with a strain of 100%, then recovered to the initial state (stage IV), in a period of 0.036 s with the vehicle speed of 0.83 m/s. The average strain rate is equal to 1/0.018 s from stage I to IV, which is 55.56 s^{-1}.

In principle, the CH-TENG can be regarded as two panel capacitors connected in series [35]. We assume the charge on the contact electrode is Q_1, the charge on the FEP film is Q, and the charge on the back electrode is Q_2. The corresponding charge densities are σ_1, σ, and σ_2. $S(t)$ is the area of contact between the FEP film and the contact electrode. ε_0 is the dielectric constant of the vacuum, and ε_r is the relative dielectric constant of the FEP film. The thickness of the FEP film is d , and the distance $x(t)$ between the contact electrode and the FEP film changes as the tire rotates.

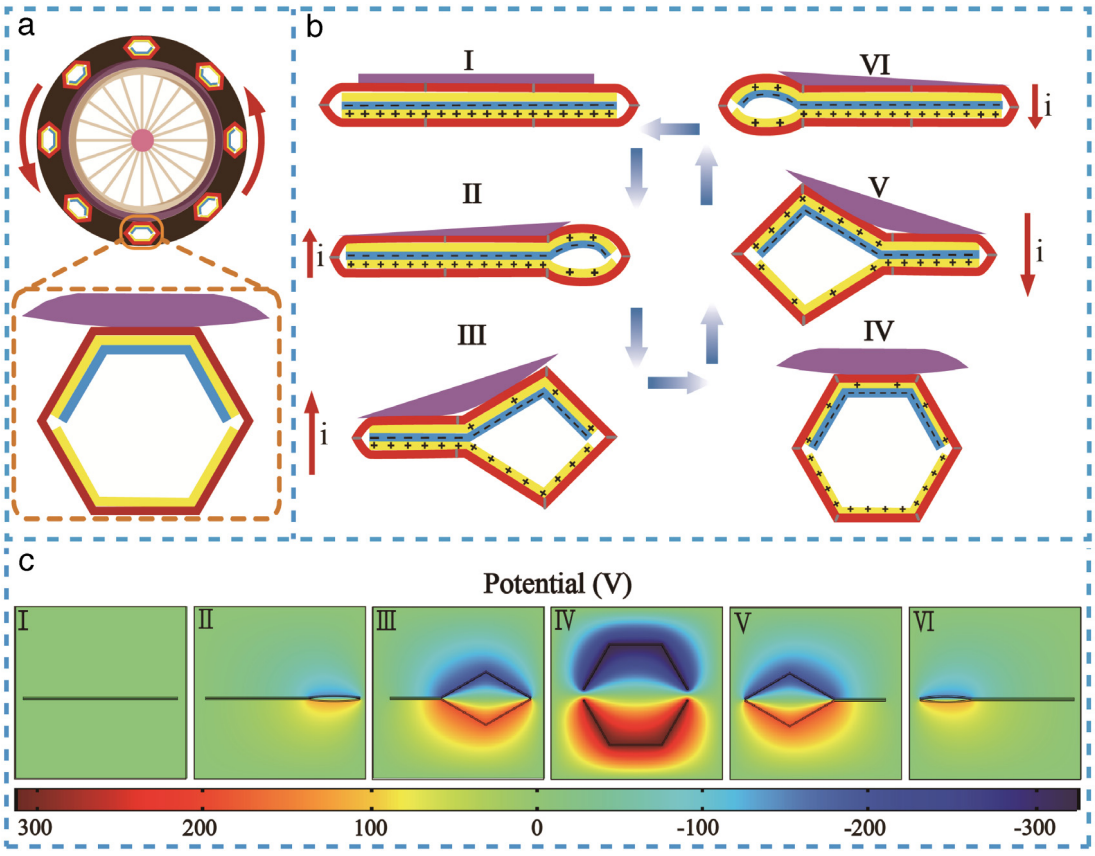

Fig. 2. Working principle of the CH-TENG in rolling tire. (a) Schematic illustration of the CH-TENG fixed in the tire. The inset is magnified schematic illustration of the CH-TENG. (b) Full cycle of the electricity generation process. (c) Numerical calculations of the potential between two electrodes at six typical states, as evaluated by COMSOL.

On the basis of electrostatic induction and conservation of charges, $Q_1 + Q_2 = -Q$. The open-circuit voltage V_{OC}, short-circuit current I_{SC} and short-circuit charge Q_{SC} can be expressed as [36]

$$V_{OC} = -\frac{\sigma x(t)}{\varepsilon_0} \tag{1}$$

$$I_{SC} = \frac{-S(t)\sigma d}{\varepsilon_r\left(\frac{d}{\varepsilon_r} + x(t)\right)^2}\frac{dx(t)}{dt} \tag{2}$$

$$Q_{SC} = \frac{S(t)\sigma x(t)}{\frac{d}{\varepsilon_r} + x(t)}. \tag{3}$$

We can see that Voc is proportional to the distance $x(t)$ by checking Eq. (1). It reaches a maximum when the FEP film and the contact electrode are furthest separated. Also V_{OC} is proportional to the triboelectric charges generated on the contacting surface, which depends on the property of the two surfaces and the friction process. It can be enhanced by choosing proper materials and modified surface morphology, as we have done in this work. By checking Eq. (2), we can conclude that the output current is proportional to the distance change rate of the two surfaces, and also proportional to the generated triboelectric charges. The distance change rate of the two surfaces is relate to the frequency of the external forces changing. By checking Eq. (3), Q_{SC} is related to distance $x(t)$ and $S(t)$.

3.3. Performances of the CH-TENG

The characteristics of the CH-TENGs are measured and shown in Fig. 3. Schematic illustration of test apparatus is shown in Fig. 3a. The test apparatus consists of a linear motor with a guide rail, acrylic boards and highly sensitive dynamometer (**Fig. S3**). The range of dynamometer is from 0 N to 50 N. With a frequency of 2.5 Hz and a weight load of 2 N, the open-circuit voltage of the CH-TENG in 1, 2, 3 and 4 units reaches 108 V, 132 V, 161 V and 190 V, respectively (Fig. 3b). In the meanwhile, the short-circuit current peak reaches 3.0 μA, 4.5 μA, 6.0 μA and 7.5 μA (Fig. 3c) and the short-circuit charge reaches 43 nC, 56 nC, 66 nC and 77 nC (Fig. 3d), respectively. Therefore, the open-circuit voltage, short-circuit current and charge increase as the number of units, as is shown in Fig. 3e. The units increasing contribute to the increase of the electric output. The specific waveforms of the open-circuit voltage, short-circuit current and charge in 4 periods are shown in **Fig. S4**. To test the instantaneous output power of the CH-TENGs in different units, different resistances are connected to the both ends of the CH-TENGs as a load. The instantaneous output power was calculated as

$$P = \frac{U^2}{R} \tag{4}$$

where R is the load resistance, P is the instantaneous output power and U is the voltage of the load resistance. The relationship of the output power P to resistance R is shown in Fig. 3f. It is evident that there exists an optimal resistive load, about 60 MΩ, 55 MΩ, 65 MΩ and 65 MΩ when the power reaches the largest value of about 0.08 mW, 0.14 mW, 0.20 mW and 0.24 mW with the CH-TENGs in 1, 2, 3 and 4 units and a load of 2 N, respectively. The peak U increased from a few volts to nearly 105 V, 130 V, 158 V and 183 V as the resistant increased to 1000 MΩ with the CH-TENGs in 1, 2, 3 and 4 units (**Fig. S5a**). Meanwhile, the peak followed an opposite trend and decreased from 3.0 μA, 4.5 μA, 6.0 μA and 7.5 μA to nearly 0 μA with the CH-TENGs in 1, 2, 3 and 4 units (**Fig. S5b**).

Fig. 4 shows performances of the CH-TENGs in the rolling tire. Considering the most relevant functions of a tire, the influences

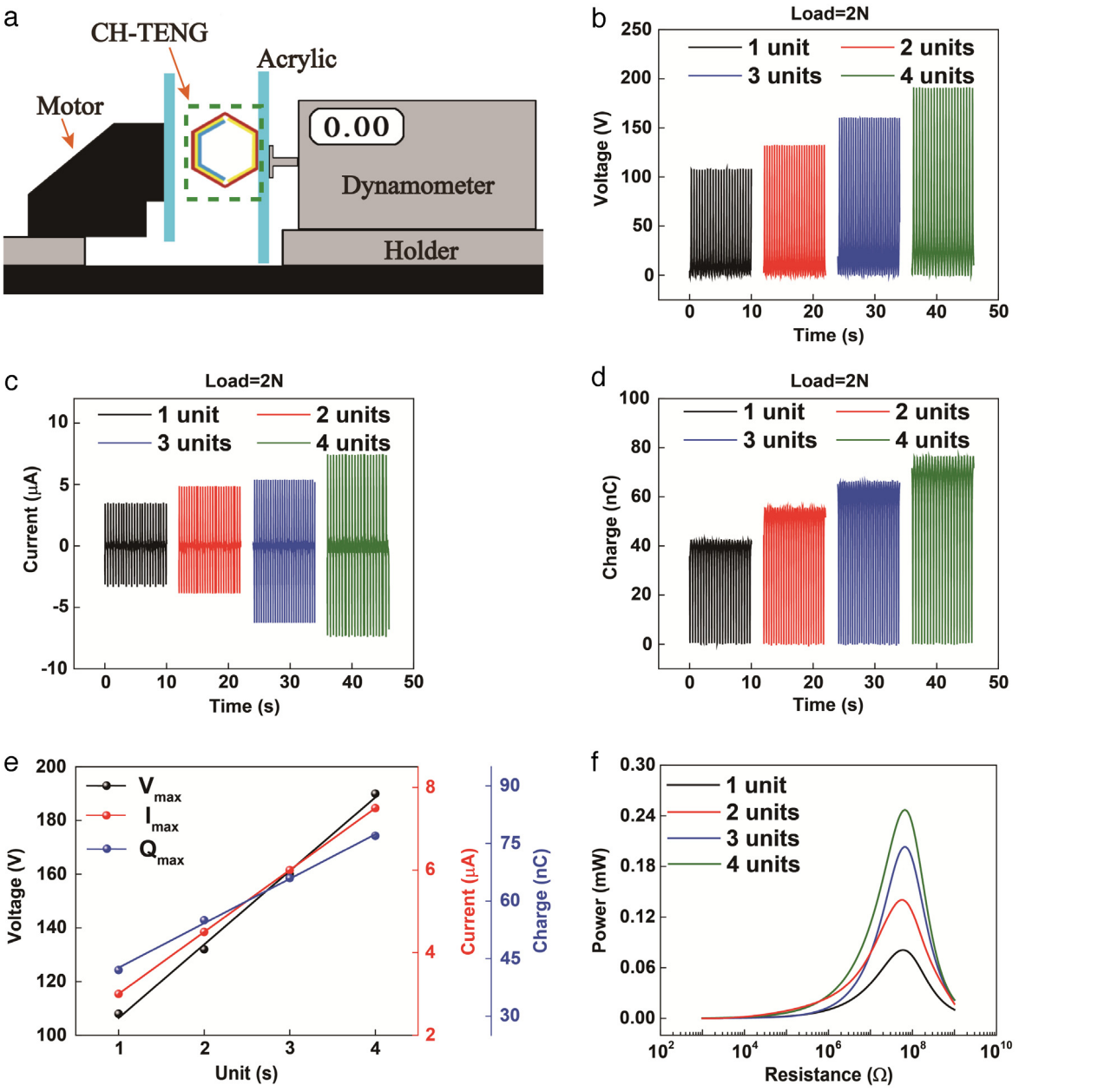

Fig. 3. Characteristics of the CH-TENGs. (a) Schematic illustration of test apparatus. The CH-TENG is compressed by linear motor. (b–d) The (b) open-circuit voltage, (c) short-circuit current and (d) short-circuit charge of the CH-TENG in 1, 2, 3 and 4 units at a frequency of 2.5 Hz and a weight load of 2 N. (e) The open-circuit voltage, short-circuit current and charge in different units. (f) The output instantaneous power as a function of the loading resistance in different units.

of moving speed and weight load of the tire on the output performances were investigated. In theory, the short-circuit current increases and the open-circuit voltage and short-circuit charge remain the same as the speed of the tire increases, also the open-circuit voltage, short-circuit current and charge increase as the weight load of the tire increases by checking Eqs. (1)–(3). The experimental design for measuring the performances of the CH-TENG in a rolling tire is schematically shown in **Fig. S6**. The CH-TENG is attached onto the surface of a rubber tire. A pair of copper foils is placed outside the tire and connected to the CH-TENG for collecting output signals. The tire is fixed on the conveyor belt by lifting platform, and the weight load can be provided to the tire by changing the height of the lifting platform. The conveyor belt is driven by a computer-controlled linear actuator, which provided linear motions at different speeds. The tire rotates with the conveyor belt. Rotating motion of the tire makes the CH-TENG on its surface periodically contacting and separating with the supporting surface. The measured average values of open-circuit voltage, short-circuit current and charge are plotted as a function of the speed of the tire as shown in Fig. 4a. The open-circuit voltage (**Fig. S7a**), short-circuit current (**Fig. S7b**) and charge (**Fig. S7c**) of the CH-TENG in 1 unit are investigated with the speed of 0.83 m/s, 1.25 m/s, 1.67 m/s, 2.09 m/s and 2.51 m/s and the weight load of 2 N. Consistent with theoretical results, the short-circuit current increases from 3.0 μA to 4.3 μA and the open-circuit voltage and short-circuit charge remain the same as the speed of the tire increases. A clear linear relationship between the short-circuit current and the speed is obtained yielding a slop of 0.892 V s m^{-1}. The frequency of electrical output with different speed is shown in **Fig. S7d**. The increasing of the short-circuit current can be attributed to the

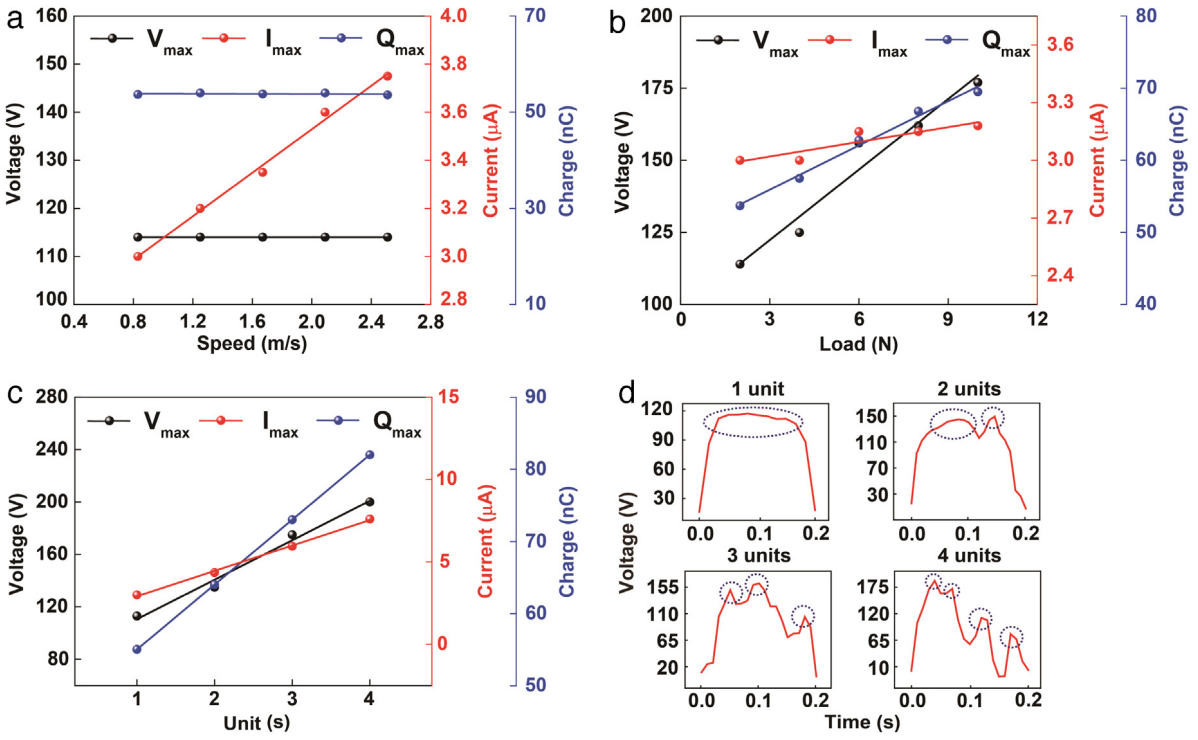

Fig. 4. Performances of the CH-TENGs in the rolling tire. (a) The open-circuit voltage, short-circuit current and charge of the CH-TENG in 1 unit with different speed and a weight load of 2 N. (b) The open-circuit voltage, short-circuit current and charge of the CH-TENG in 1 unit with different weight loads and a speed of 1.25 m/s. (c) The open-circuit voltage, short-circuit current and charge of the CH-TENG in different units with a speed of 1.25 m/s and a weight load of 2 N. (d) The feature analysis on the open-circuit voltages of the CH-TENGs in different units.

raised contacting and separation rates of the friction surfaces by checking Eq. (2). To investigate the influence of weight load on the CH-TENG's performance, a series of extra weights from 2 to 10 N are added onto the tire. Fig. 4b shows the open-circuit voltage, short-circuit current and charge of the CH-TENG in 1 unit as a function of the weight load, while the tire was moving at the same speed of 1.25 m/s. With the weight load increased from 2 to 10 N, the open-circuit voltage linearly increased from 114 V to 177 V, the short-circuit current increased from 3.0 μA to 3.2 μA, and the short-circuit charge linearly increased from 53.7 nC to 69.5 nC. From three curves, every 1 N weight load will increase the open-circuit voltage by ∼7.875 V, short-circuit current by ∼0.025 μA, short-circuit charge by ∼1.975 nC. The CH-TENGs in 1, 2, 3 and 4 units are also measured with different weight loads, as shown in **Fig. S8**. The increasing of the open-circuit voltage, short-circuit current and charges can be attributed to the raised $x(t)$ and $S(t)$ with the increasing weight load by checking Eqs. (1)–(3). Fig. 4c shows the open-circuit voltage, short-circuit current and charge of the CH-TENG in different units with a speed of 1.25 m/s and a weight load of 2 N. The open-circuit voltage, short-circuit current and charge have a growing trend as the number of the units and increase from 114 V to 200 V, 3.00 μA to 7.6 μA and 55 nC to 82 nC with the units from 1 to 4, respectively. Every one unit will increase the open-circuit voltage by ∼28.7 V, short-circuit current by ∼1.54 μA, short-circuit charge by ∼9 nC. With a speed of 1.25 m/s and a weight load of 2 N, the feature analysis on the open-circuit voltages of the CH-TENGs in different units is shown in Fig. 4d. The characteristic peak of the open-circuit voltage has a rule in the test results, in which the number of the peaks is consistent with the units. Therefore, the CH-TENG in many units with a larger speed, weight load and more units can produce more energy and harvest more mechanical energy from the tire until saturating. It is expected that the electrical output will be huger when the CH-TENGs are fixed in the tires in real vehicle. The CH-TENGs will be completely sealed in the tires and they will not affect to the friction between the tires and road.

3.4. Application of the CH-TENG

Due to the simple structures and excellent characteristics, the CH-TENGs can be integrated into the tire as the inherent part for harvesting mechanical energy with little influence on the tire structure. The CH-TENG has shown a great advantage on collecting energy from the rolling tire, and the energy can be used to drive some automotive electronics, like the wireless tire pressure sensor. In this work, we design a CH-TENG in 8 units for harvesting energy from the rolling tire to power a wireless tire pressure sensor. Photograph of the test apparatus is shown in **Fig. S9a**. Fig. 5 shows demonstration of the CH-TENGs for harvesting mechanical energy from the rolling tire and driving the wireless tire pressure sensor. The open-circuit voltage (**Fig. S9b**), short-circuit current (**Fig. S9c**) and charge (**Fig. S9d**) of the CH-TENGs in 8 units fixed in the tire are accurately measured with a speed of 2.51 m/s and a weight load of 10 N. There is a demo of a wireless tire pressure sensor, as shown by the equivalent electric circuit in Fig. 5a. The current generated by the CH-TENG is rectified to charge a capacitor and then to power a wireless tire pressure sensor which has the transmitter and the receiver. This system can be potentially applied in the automobile industry for collecting information on the tire pressure. Rated voltage and current of the tire pressure sensor are 3 V and 140 μA. The electric output of the CH-TENG in 8 units fixed in the tire is a function of the load resistance, through which the output instantaneous power can be optimized. Fig. 5b shows the resistance-dependent output voltage and power when the load resistance is swept from 100 Ω to 1000 MΩ (the wheel is moving at the same speed of 2.51 m/s with a weight load of 10 N). The output voltage increases from a few volts to nearly 490 V as the resistant increased to 1000 MΩ. Meanwhile, the instantaneous output power is calculated from Eq. (4), and plotted as a function of the resistance. The maximum output instantaneous power was found to be 1.9 mW at a load resistance of 65 MΩ. The open-circuit

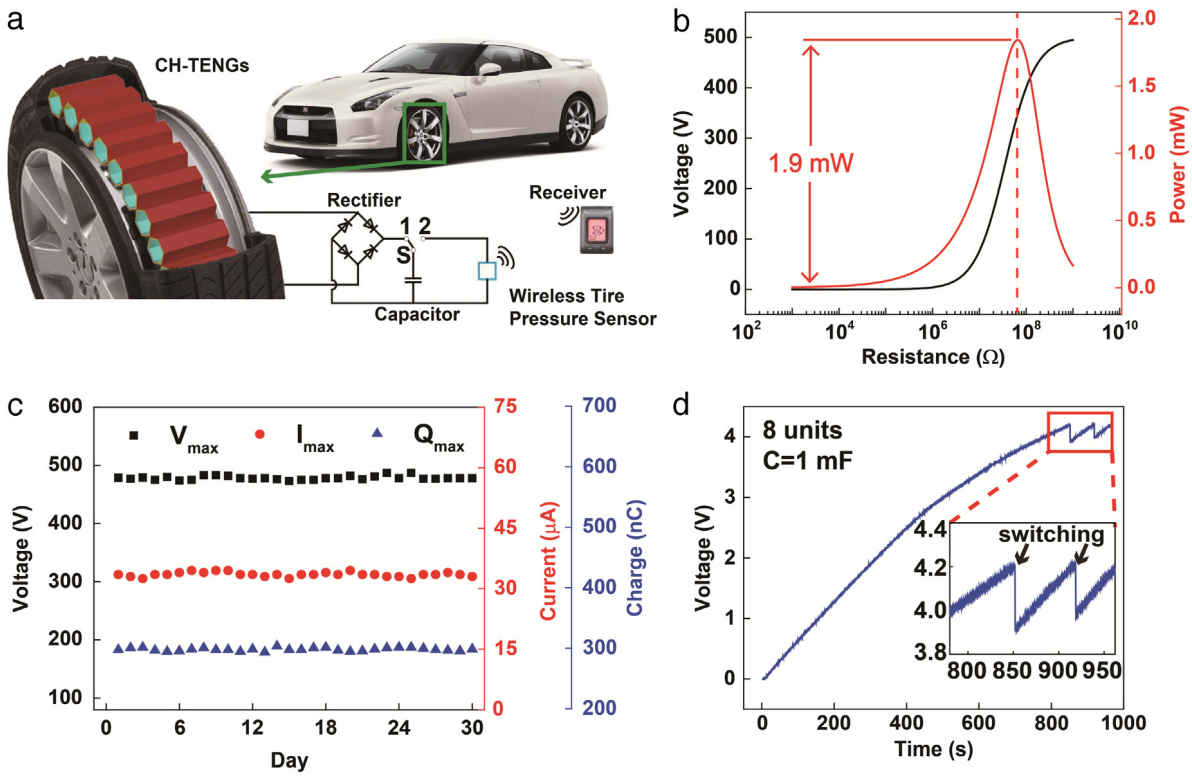

Fig. 5. Demonstration of the CH-TENGs for harvesting mechanical energy from the rolling tire and driving the wireless tire pressure sensor. (a) Equivalent electric circuit of the self-powered wireless tire pressure sensor. (b) The output voltage and instantaneous power as a function of the loading resistance in 8 units with a weight load of 10 N and a speed of 2.51 m/s. (c) The stability experiment of the CH-TENGs fixed in the tire for 30 days. (d) Charging curve for a 1 mF capacitor by the CH-TENG in 8 units in the rolling tire with a speed of 2.51 m/s and a weight load of 10 N. The inset shows the voltage drop when switching from 1 to 2.

voltage, short-circuit current and charge are measured while the tire continuously running for 30 days to investigate the stability of the CH-TENG in 8 units as shown in Fig. 5c. The open-circuit voltage, short-circuit current and charge basically keep stable at 480 V, 33 μA and 300 nC and there are no signs of large degradation or changes in the CH-TENG performance in 30 days. In addition, the nanostructures of the FEP film are degraded after the tire continuously running for 30 days with a load of 10 N. The degraded nanostructures on the surface of the FEP film have been flatted, which can be observed in the SEM image as shown in Fig. S10. However, the open-circuit voltage, short-circuit current and charge basically keep stable, which have been shown in Fig. 5c. To sum up, the degradation of the nanostructures of FEP film has little impact on the performances. Fig. 5d shows a typical charge curve at first, where the capacitor of 1 mF can be charged from 0 V to 4.2 V in about 850 s. When the wireless tire pressure sensor is turned on, the curve of voltage starts to drop and then rises again. The inset, an enlarged view, shows the voltage drop when switching from 1 to 2. The decreasing curve indicates that data is transmitted. After transmitting, the curve turns back to 3.9 V and the energy consumption is about 1.215 mJ. Movie S1 in the Supporting Information dynamically demonstrates the working process of the wireless tire pressure sensor. The CH-TENGs have shown excellent application prospect in energy harvesting from the rolling tires. If the CH-TENG (10 mm in each edge, 50 mm in width) in 500 units are equipped in a standard tire (700 mm in diameter, 250 mm in width) at the running speed is 100 km/h, as the output power of the CH-TENG in 8 units is 1.9 mW (Fig. 5b) and the output power is proportional to the movement speed [15], it is expected to produce at least 1.2 W for a standard tire, which can meet the energy demand of low-power automobile electronics, like the wireless tire pressure sensor.

4. Conclusion

In summary, we demonstrated an innovative design of CH-TENG for harvesting the mechanical energy from rolling tires. The CH-TENG units can be stacked in parallel connections and the energy harvesting performances with different unit number are systematically investigated. The open-circuit voltage and short-circuit charge of the CH-TENG fixed in the rolling tire remain unchanged as the speed of the tire increases, while the open-circuit voltage, short-circuit current and charge of the CH-TENG-on-tire increase monotonically following the increase of the weight load. By optimizing the load resistance on the external electric circuit, the maximum instantaneous power was found to be 1.9 mW at a load resistance of 65 MΩ with the CH-TENG in 8 units, a weight load of 10 N and a speed of 2.51 m/s. The CH-TENGs have stable and durable characteristics for a 30-day continuous work and can drive the wireless tire pressure sensor every 14 min when the moving speed is 2.51 m/s and weight load is 10 N. On the basis of the measured output power of the CH-TENG, it is expected to produce at least 1.2 W for a standard tire with the CH-TENG in 500 units and the running speed of 100 km/h. This work not only provides a promising solution to harvest the wasted mechanical energy from rolling tires, but also demonstrates the potential applications of the CH-TENG in sustainable automotive electronics.

Acknowledgments

Tong Guo and Guoxu Liu contributed equally to this work. The authors thank the support of National Natural Science Foundation of China (No. 51475099), Beijing Nova Program (No. Z171100001117054), the Youth Innovation Promotion Association, CAS (No. 2014033), the “thousands talents” program for

the pioneer researcher and his innovation team, China, and National Key Research and Development Program of China (2016YFA0202704).

Notes

The authors declare no competing financial interest.

Appendix A. Supplementary data

Supplementary material related to this article can be found online at https://doi.org/10.1016/j.eml.2017.10.002.

References

[1] Y. Hu, C. Xu, Y. Zhang, L. Lin, R.L. Snyder, Z.L. Wang, A nanogenerator for energy harvesting from a rotating tire and its application as a self-powered pressure/speed sensor, Adv. Mater. 23 (2011) 4068–4071.
[2] S. Zhang, Y. Wu, H. Liu, R. Huang, P. Un, Y. Zhou, L. Fu, J. Hao, Real-world fuel consumption and CO_2 (carbon dioxide) emissions by driving conditions for light-duty passenger vehicles in China, Energy 69 (2014) 247–257.
[3] Y. Wang, J. Teter, D. Sperling, China's soaring vehicle population: Even greater than forecasted? Energy Policy 39 (2011) 3296–3306.
[4] H. Huo, M. Wang, Modeling future vehicle sales and stock in China, Energy Policy 43 (2012) 17–29.
[5] Z.L. Wang, J. Chen, L. Lin, Progress in triboelectric nanogenerators as a new energy technology and self-powered sensors, Energy Environ. Sci. 8 (2015) 2250–2282.
[6] F.-R. Fan, Z.-Q. Tian, Z.L. Wang, Flexible triboelectric generator, Nano Energy 1 (2012) 328–334.
[7] Z.L. Wang, Triboelectric nanogenerators as new energy technology for self-powered systems and as active mechanical and chemical sensors, ACS Nano 7 (2013) 9533–9557.
[8] Z.L. Wang, On Maxwell's displacement current for energy and sensors: the origin of nanogenerators, Mater. Today 20 (2017) 74–82.
[9] L. Lin, Y.N. Xie, S.M. Niu, S.H. Wang, P.-K. Yang, Z.L. Wang, Robust triboelectric nanogenerator based on rolling electrification and electrostatic induction at an instantaneous energy conversion efficiency of ∼55%, ACS Nano 9 (2015) 922–930.
[10] G. Zhu, C. Pan, W. Guo, C.Y. Chen, Y. Zhou, R. Yu, Z.L. Wang, Triboelectric-generator-driven pulse electrodeposition for micropatterning, Nano Lett. 12 (2012) 4960–4965.
[11] J. Chen, G. Zhu, W. Yang, Q. Jing, P. Bai, Y. Yang, T.C. Hou, Z.L. Wang, Harmonic-resonator-based triboelectric nanogenerator as a sustainable power source and a self-powered active vibration sensor, Adv. Mater. 25 (2013) 6094–6099.
[12] G. Zhu, B. Peng, J. Chen, Q. Jing, W.L. Zhong, Triboelectric nanogenerators as a new energy technology: From fundamentals, devices, to applications, Nano Energy 14 (2015) 126–138.
[13] Y. Zi, H. Guo, Z. Wen, M.H. Yeh, C. Hu, Z.L. Wang, Harvesting low-frequency (<5 Hz) irregular mechanical energy: a possible killer application of triboelectric nanogenerator, ACS Nano 10 (2016) 4797–4805.
[14] J. Zhong, Q. Zhong, F. Fan, Y. Zhang, S. Wang, B. Hu, Z.L. Wang, J. Zhou, Finger typing driven triboelectric nanogenerator and its use for instantaneously lighting up LEDs, Nano Energy 2 (2013) 491–497.
[15] L.M. Zhang, C.B. Han, T. Jiang, T. Zhou, X.H. Li, C. Zhang, Z.L. Wang, Multilayer wavy-structured robust triboelectric nanogenerator for harvesting water wave energy, Nano Energy 22 (2016) 87–94.
[16] C. Zhang, Z.H. Zhang, X. Yang, T. Zhou, C.B. Han, Z.L. Wang, Tribotronic phototransistor for enhanced photodetection and hybrid energy harvesting, Adv. Funct. Mater. 26 (2016) 2554–2560.
[17] C. Zhang, Z.L. Wang, Tribotronics—A new field by coupling triboelectricity and semiconductor, Nano Today 11 (2016) 521–536.
[18] C. Zhang, W. Tang, L.M. Zhang, C.B. Han, Z.L. Wang, Contact electrification field-effect transistor, ACS Nano 8 (2014) 8702–8709.
[19] Y.K. Pang, X.H. Li, M.X. Chen, C.B. Han, C. Zhang, Z.L. Wang, Triboelectric nanogenerators as a self-powered 3D acceleration sensor, ACS Appl. Mater. Interfaces 7 (2015) 19076–19082.
[20] T. Zhou, Z.W. Yang, Y. Pang, L. Xu, C. Zhang, Z.L. Wang, Tribotronic tuning diode for active analog signal modulation, ACS Nano 11 (2017) 882–888.
[21] Z.W. Yang, Y. Pang, L. Zhang, C. Lu, J. Chen, T. Zhou, C. Zhang, Z.L. Wang, Tribotronic transistor array as an active tactile sensing system, ACS Nano 10 (2016) 10912–10920.
[22] Y. Pang, J. Li, T. Zhou, Z. Yang, J. Luo, L. Zhang, G. Dong, C. Zhang, Z.L. Wang, Flexible transparent tribotronic transistor for active modulation of conventional electronics, Nano Energy 31 (2017) 533–540.
[23] F. Xi, Y. Pang, W. Li, T. Jiang, L. Zhang, T. Guo, G. Liu, C. Zhang, Z.L. Wang, Universal power management strategy for triboelectric nanogenerator, Nano Energy 37 (2017) 168–176.
[24] T. Zhou, L. Zhang, F. Xue, W. Tang, C. Zhang, Z.L. Wang, Multilayered electret films based triboelectric nanogenerator, Nano Res. 9 (2016) 1442–1451.
[25] T. Zhou, C. Zhang, C.B. Han, F.R. Fan, W. Tang, Z.L. Wang, Woven structured triboelectric nanogenerator for wearable devices, ACS Appl. Mater. Interfaces 6 (2014) 14695–14701.
[26] C. Dagdeviren, Z. Li, Z.L. Wang, Energy harvesting from the animal/human body for self-powered electronics, Annu. Rev. Biomed. Eng. 19 (2017) 85–108.
[27] Y.N. Xie, S.H. Wang, L. Lin, Q.S. Jing, Z.-H. Lin, S.M. Niu, Z.Y. Wu, Z.L. Wang, Rotary triboelectric nanogenerator based on a hybridized mechanism for harvesting wind energy, ACS Nano 7 (2013) 7119–7125.
[28] C. Zhang, T. Zhou, W. Tang, C. Han, L. Zhang, Z.L. Wang, Rotating-disk-based direct-current triboelectric nanogenerator, Adv. Energy Mater. 4 (2014) 1301798.
[29] X. Zhong, Y. Yang, X. Wang, Z.L. Wang, Rotating-disk-based hybridized electromagnetic-triboelectric nanogenerator for scavenging biomechanical energy as a mobile power source, Nano Energy 13 (2015) 771–780.
[30] C. Zhang, W. Tang, C. Han, F. Fan, Z.L. Wang, Theoretical comparison, equivalent transformation, and conjunction operations of electromagnetic induction generator and triboelectric nanogenerator for harvesting mechanical energy, Adv. Mater. 26 (2014) 3580–3591.
[31] M.-H. Yeh, H. Guo, L. Lin, Z. Wen, Z. Li, C. Hu, Z.L. Wang, Rolling friction enhanced free-standing triboelectric nanogenerators and their applications in self-powered electrochemical recovery systems, Adv. Funct. Mater. 26 (2016) 1054–1062.
[32] H.L. Zhang, Y. Yang, X.D. Zhong, Y.J. Su, Y.S. Zhou, C.G. Hu, Z.L. Wang, Single-electrode-based rotating triboelectric nanogenerator for harvesting energy from tires, ACS Nano 8 (2014) 680–689.
[33] G. Zhu, Z.H. Lin, Q. Jing, P. Bai, C. Pan, Y. Yang, Y. Zhou, Z.L. Wang, Toward large-scale energy harvesting by a nanoparticle-enhanced triboelectric nanogenerator, Nano Lett. 13 (2013) 847–853.
[34] Y. Xie, S. Wang, S. Niu, L. Lin, Q. Jing, J. Yang, Z. Wu, Z.L. Wang, Grating-structured freestanding triboelectric-layer nanogenerator for harvesting mechanical energy at 85% total conversion efficiency, Adv. Mater. 26 (2014) 6599–6607.
[35] S. Niu, Z.L. Wang, Theoretical systems of triboelectric nanogenerators, Nano Energy 14 (2015) 161–192.
[36] S. Niu, S. Wang, L. Lin, Y. Liu, Y.S. Zhou, Y. Hu, Z.L. Wang, Theoretical study of contact-mode triboelectric nanogenerators as an effective power source, Energy Environ. Sci. 6 (2013) 3576–3583.